Increasing Flash Memory Lifetime by Dynamic Voltage Allocation for Constant Mutual Information

Tsung-Yi Chen, Adam R. Williamson and Richard D. Wesel
tsungyi.chen@northwestern.edu, adamroyce@ucla.edu, wesel@ee.ucla.edu

arXiv:1403.4333v1 [cs.IT] 18 Mar 2014

***Abstract*—The read channel in Flash memory systems degrades over time because the Fowler-Nordheim tunneling used to apply charge to the floating gate eventually compromises the integrity of the cell because of tunnel oxide degradation. While degradation is commonly measured in the number of program/erase cycles experienced by a cell, the degradation is proportional to the number of electrons forced into the floating gate and later released by the erasing process. By managing the amount of charge written to the floating gate to maintain a constant read-channel mutual information, Flash lifetime can be extended. This paper proposes an overall system approach based on information theory to extend the lifetime of a flash memory device. Using the instantaneous storage capacity of a noisy flash memory channel, our approach allocates the read voltage of flash cell dynamically as it wears out gradually over time. A practical estimation of the instantaneous capacity is also proposed based on soft information via multiple reads of the memory cells.**

I. Introduction

Flash memory is ubiquitous on our keychain, in our super-thin laptop, and in the racks of enterprise storage data centers. Unfortunately, Flash memory reliability degrades over time as a function of the amount of charge that is written into and subsequently erased from the memory cell. This degradation (called "wear-out") can be understood as a time-varying noise whose variance increases with the number of electrons forced into and out of the floating gate by Fowler-Nordheim tunneling. Wear-out becomes worse as the storage density (bits per memory cell) is increased by using denser constellations to store more information. The reliability and lifetime problems associated with these new, higher-density Flash memories have driven research into the use of LDPC codes to improve performance.

Fig. 1 illustrates the device structure of a NAND flash memory cell (i.e., a floating-gate transistor). To store information, a charge level is written to the cell by adding a specified amount of charge to the floating gate through Fowler-Nordheim tunneling by applying a relatively large voltage to the control gate [1]. Actually, charge is written to the floating gate incrementally with feedback, carefully approaching the desired level from below.

To read a memory cell, the charge level written to the floating gate is detected by applying a specified word-line voltage to the control gate and comparing the transistor drain current to a threshold by a sense amp comparator. If the drain current is above the comparator threshold, then the word-line voltage was sufficient to turn on the transistor, indicating that the charge written to the floating gate was insufficient to prevent the transistor from turning off. If the drain current is below the threshold, the charge written to the floating gate was sufficient to prevent the applied word-line voltage from turning on the transistor. The sense amp comparator only provides one bit of information about the charge level present in the floating gate.

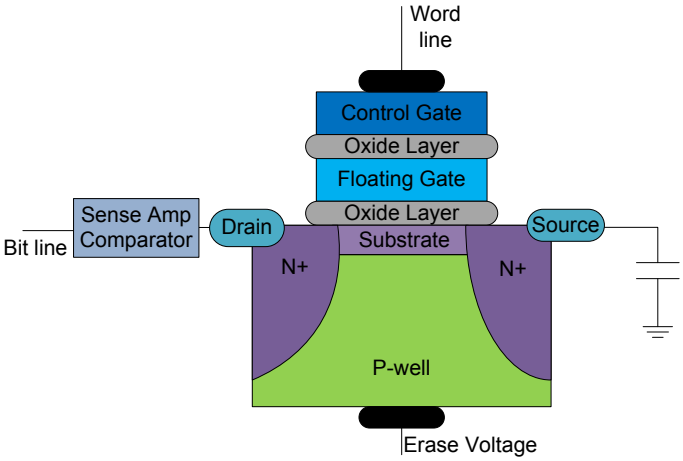

Fig. 1. NAND Flash memory cell structure.

The word-line voltage required to turn on a particular transistor is called the threshold voltage. We refer to the variation of threshold voltage from its intended value as the *read channel noise*. The threshold voltage can vary from its intended value for a variety of reasons. For example, the floating gate can be overcharged during the write operation, the floating gate can lose charge due to leakage in the retention period, or the floating gate can receive extra charge when nearby cells are written [2].

This paper presents an approach that dynamically scales the amount of charge for each level (i.e. the word-line voltage thresholds for each level) to maintain a constant mutual information over the lifetime of the device. The motivation is to increase lifetime by carefully managing the precious resource of total charge written to the cell. Our approach utilizes read-channel state information that could be provided by variable-precision decoding. Our approach maintains the simplicity of a constant instantaneous storage capacity of the device over its useful lifetime.

The rest of the paper is organized as follows: Sec. II introduces the Flash memory channel model used in this paper. Sec. III presents the main ideas of our dynamic voltage allocation and the numerical results. Sec. IV discusses practical

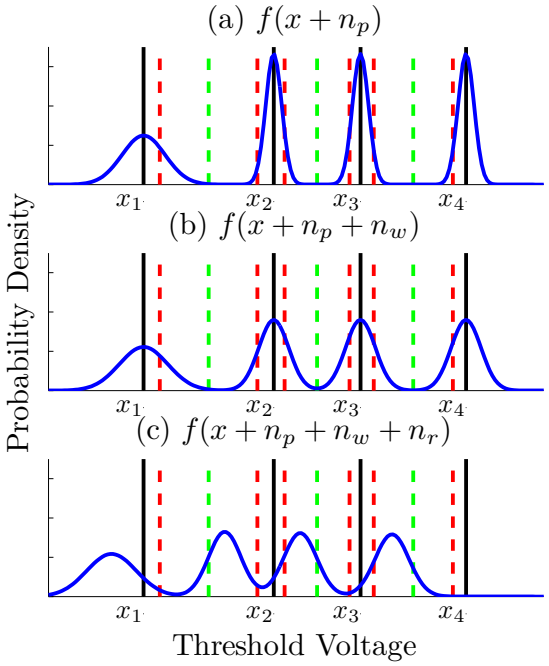

Fig. 2. Flash read channel model PDFs .

techniques to estimate the distribution of the actual Flash memory cell using multiple reads. Finally Sec. V concludes the paper.

II. Flash Memory Channel Model

This section introduces a tractable but also realistic model for Flash memory channel. Following the general approach of [3]–[7] with respect to the case of limited magnitude asymmetric errors, we first design a reasonable noise model and then seek the best possible system for that model. We draw heavily upon the extensive prior theoretical investigations and experimental studies in the semiconductor device research community [8]–[16] to capture the critical components of the time-varying and input-dependent characteristics of NAND Flash memory cells. Our model makes explicit the dependence of the wear-out and retention noise on the total amount of charge written to and subsequently erased from the memory cell. We model the NAND Flash memory cell data storage process as

$$y = x + n_p + n_w + n_r, \tag{1}$$

where x is the threshold voltage level intended to be written to the cell and y is the threshold voltage when the cell is read. The three noise components in our model are the programming noise n_p, the wear-out noise n_w, and the retention noise n_r, each of which is described in detail below. Wear-out and retention noise depend explicitly on accumulated charge.

Fig. 2 shows the contributions from each type of noise. We do not include cell-to-cell interference through parasitic capacitive coupling [17] in our model because cell-to-cell interference is a data-dependent process that can be partially mitigated by equalization and pre-distortion [18], [19]. However, the approach can be extended to handle an additional noise term reflecting residual cell-to-cell interference.

A. Programming noise

The programming noise n_p represents memory cell threshold voltage variation immediately after a brand new cell has been written. The programming noise is approximately Gaussian, but the variance is input-dependent [10], [14]. Letting x_i be the ith voltage level of a Flash cell, our model is given as

$$f_{N_p}(n_p) = \begin{cases} \mathcal{N}(0, \sigma_p^2) & \text{if } x = x_i, i > 1, \\ \mathcal{N}(0, \sigma_e^2) & \text{if } x = x_1, \end{cases} \tag{2}$$

where $\sigma_e > \sigma_p$. In other words, the erased state x_1 has a larger noise variance.

B. Wear-out noise

Flash memory program/erase (P/E) cycling causes damage (i.e., wear-out) to the tunnel oxide of Flash memory cells in the form of charge trapping in the oxide and interface states [8], [11], [20], [21]. The memory cell wear-out caused by P/E cycling is proportional to the number of electrons tunneling through the gate oxide that is further proportional to the programmed threshold voltage level. Memory cell damage caused by P/E cycling is a function of the accumulated programmed threshold voltages over these P/E cycles [21]. Let V_e denote the voltage of the erased state, $V_p^{(j)}$ denote the voltage of programmed state during the j-th P/E cycle, and N denote the total number of P/E cycles. Define the voltage accumulated over N writes as

$$V_{\text{acc}} = \sum_{j=1}^{N} (V_p^{(j)} - V_e)) \,. \tag{3}$$

Based upon the discussion and measurement results presented in [13], [22], we model the wear-out noise n_w in (1) as a Laplace $(0, \lambda)$ distribution with density $f(n_w) = \frac{1}{2\lambda} e^{-\frac{|n_w|}{\lambda}}$ with $\lambda = C_w + A_w \cdot (V_{\text{acc}}/V_{\text{max}})^{k_1}$ where constants C_w, A_w and k_1 are technology dependent with typical values around 1.26×10^{-3}, 1.80×10^{-4} and 0.62, respectively.

C. Retention noise

Retention noise n_r models the degradation of the threshold voltage integrity due to charge leakage after it is written. Interface trap recovery and electron detrapping [23]–[25] gradually reduce memory cell threshold voltages. The degradation becomes worse as V_{acc} becomes larger. Based upon the discussion and measurement results in [11], [24], the noise n_r in (1) approximately follows a Gaussian distribution $\mathcal{N}(\mu_r, \sigma_r^2)$, where the parameters μ_r and σ_r are both time-varying and voltage-dependent. Our model has mean μ_r given as

$$\mu_r = -x \ln\left(1 + \frac{t}{t_0}\right) \left[A_r \left(\frac{V_{\text{acc}}}{V_{\text{max}}}\right)^{k_1} + B_r \left(\frac{V_{\text{acc}}}{V_{\text{max}}}\right)^{k_2} \right],$$

and the variance σ_r^2 given as

$$\sigma_r^2 = 0.1x \ln\left(1 + \frac{t}{t_0}\right) \left[A_r \left(\frac{V_{\text{acc}}}{V_{\text{max}}}\right)^{k_1} + B_r \left(\frac{V_{\text{acc}}}{V_{\text{max}}}\right)^{k_2} \right]^2,$$

where x is the target threshold voltage being programmed into the memory cell. The exponents k_1 and k_1 depend on the

$$f_{Y|X}(y|x) = \frac{e^{\sigma^2/2\lambda^2}}{2\lambda}\left[\exp\left(\frac{y-\mu}{\lambda}\right)Q\left(\frac{y-\mu}{\sigma}+\frac{\sigma}{\lambda}\right)+\exp\left(\frac{-y+\mu}{\lambda}\right)Q\left(\frac{-y+\mu}{\sigma}+\frac{\sigma}{\lambda}\right)\right]. \quad (4)$$

manufacturing technology of the devices. In the current paper we choose $k_1 = 0.62$ and $k_2 = 0.3$. The constants A_r and B_r are technology dependent with typical values around 7.0×10^{-4} and 4.76×10^{-3}, respectively, and t_0 is the time constant that also depends on the manufacturing technology.

III. Dynamic Voltage Allocation Based on Mutual Information

As discussed in Sec. II, the noise of a Flash cell can be modeled as a sum of Gaussian and Laplacian random variables with time-varying parameters. A similar channel model has been studied in the context of multiple-user communication with impulse radio [26], [27]. Our model channel has the overall conditional distribution given as (4), shown at the top of the page, where $\sigma^2 = \sigma_p^2 + \sigma_r^2$, $\mu = \mu_r + x$ and $Q(x)$ is the tail of the standard Gaussian random variable:

$$Q(x) = \int_x^\infty \sqrt{2\pi}\exp\{-x^2/2\}.$$

With a uniform input distribution for an L-level Flash cell (L equally likely inputs), the distribution of the channel output is given as

$$f_Y(y) = \sum_{i=1}^{L} f_{Y|X}(y|x_i)/L,$$

where x_i is the ith voltage level and x_1 represents the erased state. Recall that the programming noise variance is larger than all other states as discussed in Sec. II.

For a given voltage level, we can calculate the relevant mutual information (the highest theoretical information rate for equally likely inputs) according to the expected accumulated voltage $\mathbb{E}[V_{\text{acc}}] = \mathbb{E}[\sum_{j=1}^{N} V_p^{(j)} - V_e]$ and a specified maximum retention time. This is the *instantaneous storage capacity* of a Flash cell and the total storage capacity is this value scaled by the number of cells.

In practice, a margin between the actual channel coding rate and capacity is necessary to provide a reliable error protection. The smallest possible margin for a specified block length can be found using the finite-blocklength analysis in [28]. Specifically, for a given reliability of ϵ and the channel code's blocklength n, we can find the least margin required to achieve by using the finite-blocklength converse. The normal approximation formula in [28] is given as

$$nR = nC - \sqrt{nV}Q^{-1}(\epsilon) + O(\log n) \quad (4)$$

where C is the channel capacity and V is the channel dispersion . This approximation can serve as a coarse assessment of the margin between the channel coding rate and the capacity of a general Flash memory channel.

For practical high-rate LDPC codes on a Gaussian channel model, we observe experimentally that typical margins are around 0.1 to 0.15 bits. Once the average value of $E[V_{\text{acc}}]$ over a group of cells is large enough that the instantaneous capacity is less than the code rate plus the needed margin, the code will fail to provide reliable error protections over that group of cells.

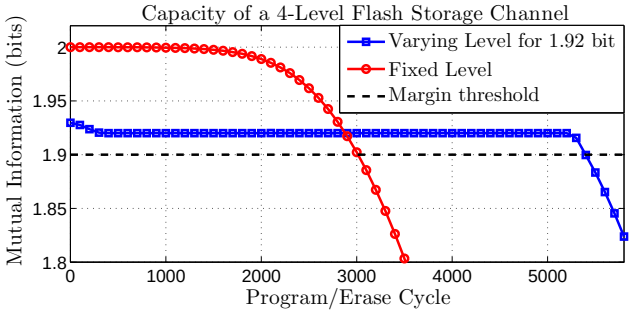

Fig. 3. Capacity vs. P/E cycle at 1 year retention time.

There is a tension between the instantaneous capacity and the lifetime of a cell; higher voltage levels provide higher instantaneous capacity but causes the Flash cells to wear out faster. One possible approach is to use constant voltage levels and variable rate coding to decrease the rate as the instantaneous capacity decreases. However, both USB drives and enterprise storage applications tend to assume that the instantaneous storage capacity remains constant over the lifetime of the device.

Our approach recognizes that the device needs to maintain a specified instantaneous storage capacity and designs the system to maximize the lifetime over which that capacity is maintained. This does not preclude the use of variable-rate coding to allow the device to be of use during its "after life", but the goal is to delay this as long as possible. We use information theory to dynamically tune the voltage levels to maintain only the needed margin, minimizing V_{acc}. This achieves a longer average lifetime. The extremely large margin common in the beginning of a cell's life is not needed (since the LDPC code is in place) and that excess margin comes at the cost of a shorter lifetime.

To illustrate this, take a Flash chip with 4-level cells as in Fig. 2 and a rate-$8/9$ error correction code as an example. Suppose the needed margin of 0.12 bits requires the instantaneous capacity to be above 1.9 bits. For this example, the technology-dependent parameters are chosen as follows: $A_w = 1.8\times 10^{-4}$, $C_w = 1.26\times 10^{-3}$, $A_r = 7.0\times 10^{-4}$, $B_r = 4.76\times 10^{-3}$, $V_{\max} = 16$. The voltage levels are set to be $\{2.8, 5.2, 6.4, 7.86\}$. The time constant is set to $t_0 = 1$ (in units of hours). The state-dependent Gaussian noise variances are chosen to be $\sigma_p = 0.05$ and $\sigma_e = 0.35$.

For a retention time of 1 year ($t = 8760$ hours), the red curve in Fig. 3 is the baseline for fixed voltage levels over the lifetime. The baseline voltage levels are chosen such that the instantaneous capacity drops to 1.9 bits at a typical lifetime of 3000 P/E cycles for a 4-level Flash cell. Fig. 3 also shows the instantaneous capacity using our dynamic voltage level

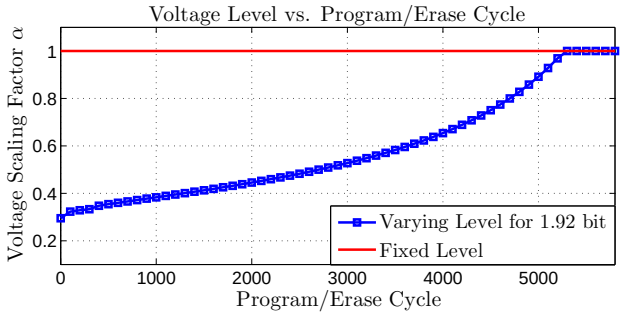

Fig. 4. α vs. P/E cycle at 1 year retention time.

approach. The voltage levels are scaled by a single parameter α, adjusted after every 100 P/E cycles to attain instantaneous capacity of 1.92 bits (slightly higher than the threshold to provide extra margin) until the voltage levels become the same as our baseline ($\alpha = 1$). This single parameter scheme improves the lifetime from 3000 to 5400 P/E cycles: an 80% improvement in this example.

Fig. 4 compares α as a function of P/E cycles between the varying level scheme and the baseline. The initial α is set to 0.28 and as the device wears out, α is gradually increased to match the desired mutual information margin every 100 P/E cycles. As illustrated in Fig. 4, the lifetime improvement is significant since a brand new Flash cell only needs 28% of the fixed voltage levels to achieve sufficient amount of instantaneous capacity. Fixed voltage levels waste 70% of the early voltage, needlessly damaging the Flash cell. We emphasize that this is only an initial illustration. Investigation of a variety of ways to improve performance further including optimizing the frequency of charge level adjustment and more carefully optimizing each of the charge levels is ongoing work.

IV. Assessment of Wear-Out and Retention Noise

Our dynamic-voltage-level approach determines at regular (though infrequent) intervals how much to increase the voltage levels. At each channel assessment period, we can numerically solve the general optimization problem of where to place each level to achieve the desired instantaneous capacity with the least growth in V_{acc}. This requires the ability to assess the wear-out condition of a page. However, this can be accomplished using the same approach that is used to generate soft information for LDPC decoding [29].

Estimation of a true distribution from an empirical distribution (or a quantized empirical distribution) is a well known technique. Fig. 5 shows the histogram of threshold voltage regions identified by simulated reading of 9000 4-level MLC Flash memory cells using the word-line voltage model as discussed above and shown in Fig. 2. The vertical dashed lines in the three threshold voltage distributions shown in Fig. 2 are used to produce the histograms in Fig. 5. These would also be the thresholds used in the limited-precision soft information [29] used by the decoder for two codewords of a rate-$8/9$ LDPC code each protecting 1 kilobyte of information on a page in memory stored on these 9000 cells. Thus, the mechanism to produce this histogram information is already

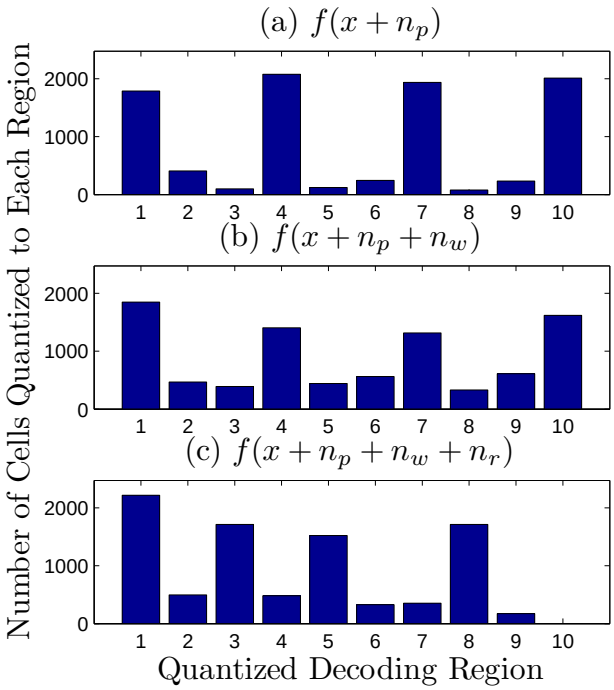

Fig. 5. Histogram of 9000 Flash cells with threshold voltage distributions and memory-sensing word-line voltages as shown in Fig. 2

available in Flash memory utilizing multiple reads to obtain soft information for decoding LDPC codes.

Figs. 5 (a) and (b) indicate that the degree of wear-out faced by a page in Flash memory can be estimated from such a histogram with enough accuracy to support the dynamic voltage level approach. We note that in [30] the author uses a similar histogram approach to estimate the threshold voltage distribution for the purpose of choosing the best possible quantization thresholds according to [29]. In [30], twelve histogram bins were sufficient to estimate with high precision the means and variances of a mixture of four Gaussians. Thus, the method of distribution estimation from the histogram is sound.

While information theoretic analysis provides the foundation for this approach, our implementation is practical. The histogram is generated immediately after a write to avoid confusion with retention loss effects. Then, whether and how much to increase voltage levels can be determined as a function of how many threshold voltages are outside of the "correct" bins. This approach can be applied on a block-by-block basis so that constant mutual information can be maintained despite the large variations that have been observed between blocks.

The histogram approach can also identify and largely mitigate the mean-shift portion of retention loss. Comparing Figs. 5 (b) and (c) shows the mean shift due to retention loss as a left-shift of the most populated bins, which affects LDPC decoding. This was also observed in [30], where a second cycle of memory sensing follows the histogram-estimated means and variances to obtain optimal limited-precision soft information. We explore an alternative approach that uses the obtained histogram to adjust how likelihood ratios are assigned to the

histogram bins.

The example of Figs. 2 and 5 only considered three quantization thresholds between two adjacent storage levels for simplicity. Commercial NAND Flash memory chips already support more levels. The Samsung 21nm 2 bits/cell chip can support six quantization thresholds between two adjacent storage states [31]. Thus we are confident that the mechanism for generating sufficiently rich histograms will exist as a matter of course in future Flash memory systems.

V. Conclusion

Using information theory, we have introduced a novel dynamic voltage allocation method to increase the lifetime of a Flash storage device. A channel model based on voltage-dependent Gaussian noise and Laplace noise is used to demonstrate the numerical results, our idea is applicable to general Flash memory channel model. For the parameters chosen in this paper, the dynamic voltage allocation almost doubles the lifetime of a 4-level Flash memory cell. We expect additional lifetime extension for a general Flash memory channel model.

In order to obtain the (approximate) mutual information of the Flash memory channel, the noise distribution must be available. We propose estimating the noise distribution by using the quantized soft information obtained during the page-reading process, which is an emerging feature in modern Flash memory devices.

References

[1] R. Bez, E. Camerlenghi, A. Modelli, and A. Visconti, "Introduction to Flash Memory," *Proc. IEEE*, vol. 91, no. 4, April 2003.

[2] Y. Maeda and K. Haruhiko, "Error Control Coding for Multilevel Cell Flash Memories Using Nonbinary Low-Density Parity-Check Codes," in *24th IEEE Int. Symp. on Defect and Fault Tolerance in VLSI Systems*, Chicago, IL, Oct. 2009.

[3] N. Elarief and B. Bose, "Optimal, systematic, q-ary codes correcting all asymmetric and symmetric errors of limited magnitude," *IEEE Trans. Inf. Theory*, vol. 56, no. 3, pp. 979–983, March 2010.

[4] T. Klove, J. Luo, I. Naydenova, and S. Yari, "Some codes correcting asymmetric errors of limited magnitude," *IEEE Trans. Inf. Theory*, vol. 57, no. 11, pp. 7459–7472, Nov. 2011.

[5] T. Klove, B. Bose, and N. Elarief, "Systematic, single limited magnitude error correcting codes for flash memories," *IEEE Trans. Inf. Theory*, vol. 57, no. 7, pp. 4477–4487, July 2011.

[6] N. Elarief, B. Bose, and S. Elmougy, "Limited magnitude error detecting codes over Z_q," *IEEE Trans. Comput.*, vol. 62, no. 5, pp. 984–989, May 2013.

[7] Y. Cassuto, M. Schwartz, V. Bohossian, and J. Bruck, "Codes for asymmetric limited-magnitude errors with application to multilevel flash memories," *IEEE Trans. Inf. Theory*, vol. 56, no. 4, pp. 1582–1595, April 2010.

[8] P. Olivo, B. Ricco, and E. Sangiorgi, "High Field Induced Voltage Dependent Oxide Charge," *Applied Physics Letter*, vol. 48, pp. 1135–1137, 1986.

[9] D. Wellekens, J. Van Houdt, L. Faraone, G. Groeseneken, H. Maes, and L. IMEC, "Write/erase degradation in source side injection flash EEPROM's: Characterization techniques and wearout mechanisms," *IEEE Trans. on Electron Devices*, vol. 42, no. 11, pp. 1992–1998, 1995.

[10] K. Takeuchi, T. Tanaka, and H. Nakamura, "A double-level-Vth select gate array architecture for multilevel NAND flash memories," *IEEE Journal on Solid-State Circuits*, vol. 31, no. 4, pp. 602–609, Apr. 1996.

[11] N. Mielke, H. Belgal, I. Kalastirsky, P. Kalavade, A. Kurtz, Q. Meng, N. Righos, and J. Wu, "Flash EEPROM threshold instabilities due to charge trapping during program/erase cycling," *IEEE Trans. on Device and Materials Reliability*, vol. 4, no. 3, pp. 335–344, 2004.

[12] J. Lee, J. Choi, D. Park, K. Kim, R. Center, S. Co, and S. Gyunggi-Do, "Effects of interface trap generation and annihilation on the data retention characteristics of flash memory cells," *IEEE Trans. on Device and Materials Reliability*, vol. 4, no. 1, pp. 110–117, 2004.

[13] K. Fukuda, Y. Shimizu, K. Amemiya, M. Kamoshida, and C. Hu, "Random telegraph noise in flash memories - model and technology scaling," in *Proc. of IEEE International Electron Devices Meeting (IEDM)*, Washington, DC, 2007, pp. 169–172.

[14] C. Compagnoni, A. Spinelli, R. Gusmeroli, A. Lacaita, S. Beltrami, A. Ghetti, and A. Visconti, "First evidence for injection statistics accuracy limitations in NAND Flash constant-current Fowler-Nordheim programming," in *Proc. of IEEE International Electron Devices Meeting*, 2007, pp. 165–168.

[15] A. Ghetti, C. Compagnoni, F. Biancardi, A. Lacaita, S. Beltrami, L. Chiavarone, A. Spinelli, and A. Visconti, "Scaling trends for random telegraph noise in deca-nanometer flash memories," in *Proc. of IEEE International Electron Devices Meeting (IEDM)*, San Francisco, CA, 2008, pp. 1–4.

[16] A. Spinelli, C. Compagnoni, R. Gusmeroli, M. Ghidotti, and A. Visconti, "Investigation of the random telegraph noise instability in scaled Flash memory arrays," *Japanese Journal of Applied Physics-Part 1 Regular Papers and Short Notes*, vol. 47, no. 4, pp. 2598–2601, 2008.

[17] J.-D. Lee, S.-H. Hur, and J.-D. Choi, "Effects of Floating-Gate Interference on NAND Flash Memory Cell Operation," *IEEE Electron Device Letters*, vol. 23, no. 5, pp. 264–266, May. 2002.

[18] Y. Li and Y. Fong, "Compensating for coupling based on sensing a neighbor using coupling," *United States Patent 7,522,454*, Apr. 2009.

[19] G. Dong, S. Li, and T. Zhang, "Using data post-compensation and pre-distortion to tolerate cell-to-cell interference in MLC NAND flash memory," *Transactions on Circuits and Systems-I: Regular Papers*, vol. 57, no. 10, pp. 2718–2728, 2010.

[20] P. Cappelletti, R. Bez, D. Cantarelli, and L. Fratin, "Failure mechanisms of flash cell in program/erase cycling," in *Proc. of International Electron Devices Meeting (IEDM)*, 1994, pp. 291–294.

[21] S. Yamada, Y. Hiura, T. Yamane, K. Amemiya, Y. Ohshima, and K. Yoshikawa, "Degradation mechanism of flash EEPROM programming afterprogram/erase cycles," in *Proc. of International Electron Devices Meeting (IEDM)*, 1993, pp. 23–26.

[22] C. Compagnoni, M. Ghidotti, A. Lacaita, A. Spinelli, and A. Visconti, "Random telegraph noise effect on the programmed threshold-voltage distribution of flash memories," *IEEE Electron Device Letters*, vol. 30, no. 9, 2009.

[23] N. Mielke, H. Belgal, A. Fazio, Q. Meng, and N. Righos, "Recovery Effects in the Distributed Cycling of Flash Memories," in *Proc. of IEEE International Reliability Physics Symposium*, 2006, pp. 29–35.

[24] H. Yang, "Reliability Issues and Models of sub-90nm NAND Flash Memory Cells," in *Proc. of International Conference on Solid-State and Integrated Circuit Technology*, Shanghai, China, 2006, pp. 760–762.

[25] J. Lee, J. Choi, D. Park, and K. Kim, "Data retention characteristics of sub-100 nm NAND flash memory cells," *IEEE Electron Device Letters*, vol. 24, no. 12, pp. 748–750, 2003.

[26] M. Win and R. Scholtz, "Ultra-wide bandwidth time-hopping spread-spectrum impulse radio for wireless multiple-access communications," *IEEE Trans. Commun.*, vol. 48, no. 4, pp. 679 –689, Apr 2000.

[27] N. Beaulieu and S. Niranjayan, "UWB receiver designs based on a gaussian-laplacian noise-plus-MAI model," *IEEE Trans. Commun.*, vol. 58, no. 3, pp. 997 –1006, Mar 2010.

[28] Y. Polyanskiy, H. Poor, and S. Verdú, "Channel coding rate in the finite blocklength regime," *IEEE Trans. Inf. Theory*, vol. 56, no. 5, pp. 2307 –2359, May 2010.

[29] J. Wang, K. Vakilinia, T.-Y. Chen, T. Courtade, G. Dong, T. Zhang, H. Shankar, and R. D. Wesel, "Enhanced precision through multiple reads for LDPC decoding in flash memories (to appear)," *IEEE J. Sel. Areas Commun.*, 2014. [Online]. Available: http://arxiv.org/abs/1309.0566v4

[30] D.-H. Lee and W. Sung, "Estimation of NAND flash memory threshold voltage distribution for optimum soft-decision error correction," *IEEE Trans. Signal Process.*, vol. 61, no. 2, pp. 440–449, Jan 2013.

[31] C. Kim, J. Ryu, T. Lee, H. Kim, J. Lim, J. Jeong, S. Seo, H. Jeon, B. Kim, I. Lee, D. Lee, P. Kwak, S. Cho, Y. Yim, C. Cho, W. Jeong, K. Park, J.-M. Han, D. Song, K. Kyung, Y.-H. Lim, and Y.-H. Jun, "A 21 nm high performance 64 Gb MLC NAND flash memory with 400 MB/s asynchronous Toggle DDR interface," *IEEE J. of Solid-State Circuits*, vol. 47, no. 4, pp. 981–989, April 2012.